Zaria Journal of Electrical Engineering Technology, Department of Electrical Engineering, Ahmadu Bello University, Zaria – Nigeria. Vol. 10 No. 2, Month 2021. ISSN: 0261 – 1570.

DEVELOPMENT OF AN IMPROVED PILOT DECONTAMINATION SCHEME USING ORTHOGONAL UPLINK PILOT SEQUENCE BASED ON LARGE SCALE FADING MASSIVE MIMO SYSTEMS

[1]S. M. Atiku, [2]A. M. S. Tekanyi, [3]K. A. Abubilal, H. A. Abdulkareem, and U. F. Abdu-Ague
Department of Communications Engineering,Ahmadu Bello University,Zaria – Nigeria.
atikushe1@gmail.com,

Keywords: –
Keywords
M-MIMO, Pilot Contamination, OVSF, and ZCPS

Article History: –
Received: March, 2021.
Reviewed: June, 2021
Accepted: August, 2021
Published: September, 2021.

ABSTRACT

Pilot contamination (PC) is the major challenge in Massive Multiple Input Multiple Output (M-MIMO) systems of work of previous researchers because it reduces the achievement of numerous benefits of the M-MIMO system. In this proposed scheme, users are classified into center cell and edge cell users based on their large-scale fading. The center cell users suffer less or no interference which not the case with the edge cell users. Pilot sequences are assigned to the center cell users, which are shared sequentially with new users after being exhausted. The edge cell users are assigned distinct Orthogonal Variable Spreading Factor (OVSF) and multiplied then by Zadoff Chu Pilot Sequence (ZCPS), thereby creating orthogonality across the cells as well as across the neighboring cells. This process reduces or eliminates interference, resulting in improved performance of the M-MIMO system as evident from both the plots of the results of the work of Ali et al., (2017a) and that of the developed scheme. When the plots of the sum-rate against standard deviation of AoA, number of antennae, cross gain, and number of cells of both schemes are compared, the developed scheme outperformed the existing work with improvements of 6.8%, 11.11%, 12.20%, and 11.90%, respectively.

1. INTRODUCTION

The growing need for higher data rates in the system of wireless communication have necessitate the requirement for innovative technologies that is competent in the provision of high capacity in contrast with previous mobile network technologies (Elijah *et al.*, 2016). It was predicted that, there would be a serious rise in mobile communication traffic through the next decade, therefore, the next Fifth Generation (5G) network demand arouse in order to achieve the predicted capacity (Li *et al.*, 2014). Massive Multiple-Input Multiple-Output (M-MIMO) systems have been predicted to be the technology to cater for this large data capacity for mobile network (Elijah *et al.*, 2016). In addition, 5G network is capable of solving the shortcomings associated with the previous communication systems, such as multi-media applications, reliability of the link, latency, full coverage, and energy efficiency (Larsson *et al.*, 2014).

When an extra data of pilot is transmitted together with actual signal, it helps in the determination of Channel State Information (CSI). The multi-cell M-MIMO systems suffer from Pilot Contamination (PC). PC interference that occurs as a result of pilot sequence reuse in the nearby cells in the course of channel estimation which cannot be overcome with the increasing number of antenna is the major challenge in M-MIMO systems (Muppirisetty *et al.*, 2018).

The Least Square (LS) channel estimator which does not require perfect knowledge of channel statistics results to estimates not good enough,while Minimum Mean Square Error (MMSE) estimator which requires the ideal knowledge of channel covariance matrix gives better estimates (Mehrotra & Chaubey, 2017). Numerous schemes have been suggested in the literature as an effort to resolve the problem of PC in multi cell M-MIMO system (Liu *et al.*, 2017). Considering the issues of CSI estimation error in multi-cell system, Benmimoune *et al.*, (2015) projected an integer linear programming and heuristic dynamic programming algorithm, while Tebe *et al.*, (2015) suggested down link transmit power model. Despite this effort, there is still the need for improvement in terms of sum-rate capacity through PC reduction, CSI estimation improvement, pilot sharing technique, and improved fading channel model (like Nakagami fading channel model).

2. REVIEW OF SIMILAR WORK

Salh*et al.*, (2020) proposed the mitigation of pilot contamination for channel estimation in multi-cell M-MIMO systems, a technique that reduced PC and improved the performance of edge cell users through the use of the large scale fading and orthogonal pilot sequence reuse. The edge cells PC issue was eliminated using, Matched Filter (MF) and Zero Forcing (ZF) pre-coding scheme. The system's results could be better, if the MMSE pre-coder is employed because of its better performance.

Waziri*et al.*, (2019) proposed the development of Pilot Allocation Protocol (PAP) for the mitigation of PC and enhancement of edge cell users' performance in Time Division Duplex (TDD) M-MIMO systems. Sectional pilot sequence sharing was employed and the Rayleigh fading channel was used for initialization. In the scheme, more than one user shared the same orthogonal pilot sequence. Signal equalization was achieved by using ZF and MF pre-coding/detection scheme. It was verified that ZF out performed MF in terms of Bit Error Rate (BER). There is need for further intervention in the edge cell user's orthogonality to further enhance the overall system performance as well as achieve better sum rate capacity.

A scheme based on location was projected by Muppirisetty et al., (2018) to reduce PC in the uplink transmission of M-MIMO systems. The scheme made use of inexact location of UT including their BS in order to present fine estimate of the CSI between UT and their matching BSs. The system was designed to avoid PC in the presence of moderate number of transmission antennae and assigned identical pilot sequences to several users from different or the same cell. Pilot coordination technique for multi-user multi cell system was suggested for pilot decontamination. The results from this technique showed that there was improvement in the overall sum-rate. Despite the tremendous achievement in the overall sum rate, the cost of coordination was the major drawback of this study.

Ali *et al.*, (2017a) proposed the development of orthogonal uplink pilot sequences for multi-cell TDD

M-MIMO system. Zadoff-Chu Pilot Sequence (ZCPS) was employed in order to eliminate PC during channel estimation. In this proposed method, there was assignment of definite orthogonal code to individual Base Station (BS) followed by the multiplication of ZCPS element-wise at individual BS, which created orthogonality across the nearby cells. The simulation results showed that this proposed design got rid of PC for the period of channel estimation procedure, thereby improving the sum rate gains. Large scale fading was not considered in this technique which could have affected the results.

2.1 Review of Concepts

It is important to review models, tools, methods, and techniques used in addressing problems associated with PC. This equips the researcher with the adequate knowledge suitable to make appropriate choices on these aspects necessary to obtain better results.

2.1.1 Uplink Training Model

Considering a BS q, the received uplink signal (y_q) is modeled as in Ali *et al.*, (2017):

$$Y_q = \sqrt{\rho_{up}} \sum_{l=1}^{L} \sqrt{D_{lq}}\, H_{lq} Z + V_q \qquad (1)$$

where, ρ_{up} denotes the average uplink transmit power, D_{lq} is given by $diag\,(\beta_{lq1},\ \beta_{lq2},\ldots\ \beta_{lqU})$,$\beta_{lqU}$ represents the cross gain, H_{lq} corresponds to the channel coefficient, Z depicts the set of pilot sequences (Z_1, Z_2 ... Z_U), and V_q stands for Additive White Gaussian Noise (AWGN).

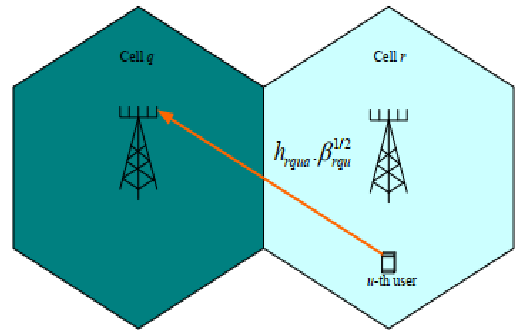

Figure 1: The model of connection between the *a*-th antenna of the *q*-th cell and *u*-th user of the *r*-th cell in a TDD M-MIMO System ali et al, (2017a)

2.1.2 Downlink Transmission

The downlink transmission is achieved by employing the Minimum Mean Square Error (MMSE) pre-coder. due to its lesser noise and interference with high power efficiency advantages over other pre-coding techniques (Albreem *et al.*, 2019). The MMSE pre-coder and the corresponding output from the MMSE are mathematically modeled as follows(Albreem *et al.*, 2019):

$$A_{MMSE}^{H} = (H^H H + \frac{K}{SNR} I)^{-1} H^H \quad (2)$$

$$\hat{X}_{MMSE} = S(A_{MMSE}^{H} y) \qquad (3)$$

where, I stands for the identity matrix, H^T denotes the transpose of the channel matrix, H^H is the Hermitian channel matrix, $H^H H$ represents the Grammian matrix, $S(.)$, the slicer quantizes each entry to the nearest neighbor in the constellation, and K corresponds to the number of mobile users.

The achievable rate with MMSE pre-coder for the uplink and downlink is given by Fatema *et al.*, (2017):

$$\hat{h}_{qqa}^{MMSE} = \sqrt{\rho_{up}}\beta_{qq}\big(I + \rho_{up}(\textstyle\sum_{l=1}^{L}\sum_{u=1}^{U} C_q \beta_{lqu} C_q^H)\big)^{-1} y_q C_q^H \qquad (4)$$

where, C_q corresponds to the pilot sequence and C_q^H represents the Hermitian transpose of the pilot sequence, β_{lqu} is the cross gain,β_{qq}denotes the direct gain, $y_q$stands for the received signal, Ldepicts the number of cells, and $u$signifies the number of users. The Angle of Arrival (AoAs) $\theta_{lqu}$of all paths are independent and identically distributed (iid) Gaussian random variables with mean $\theta_{AoA} = 90^0$ and standard deviation $\sigma_{AoA} = 90^0$. The larger the number of Antenna (A), the higher the sum-rate and the propagation diversity gain of the system(Ali et al., 2017b).

2.1.3 Zadoff–Chu Pilot Sequences (ZCPS)

Zadoff-Chu sequences have vast applications, but are mainly employed as reference signal (pilot) in order to provide good timing estimation due to their better autocorrelation property (that is, their Constant Amplitude and Zero Auto Correlation (CAZAC) property). Hence, it is believed that Zadoff Chu (ZC) sequence may be employed as the pilot sequence in the next generation networks (Ali *et al.*, 2017a) and it is modeled in Ali *et al.*, (2017) as:

$$Z_\mu(n) = e^{-j\pi\mu\frac{n^2}{P}}, n = 0,1, \dots . P - 1 \qquad (5)$$

where, P is the pilot sequence length (even), $\mu \in (1,2, \dots, P - 1)$represents the pilot sequence root index.

2.1.4 Orthogonal Codes

Orthogonal codes are classified into three, mainly: Walsh, Hadamard, and OVSF (Rintakoski *et al.*, 2004). The common orthogonal codes such as OVSF and Hadamard codes are often employed in pilot sequence designs(Tseng & Chao, 2002). There is mutual orthogonality in the code rows of these codes. Therefore, multiplying the code rows element-wise with ZC pilot sequence creates orthogonality across the network (Tseng & Chao, 2002).

Consider an 8 by 8 orthogonal matrix as follows (Ali *et al.*, 2017a):

$$O_8 = \begin{vmatrix} 1 & 1 & 1 & 1 & 1 & 1 & 1 & 1 \\ 1 & 1 & 1 & 1 & -1 & -1 & -1 & -1 \\ 1 & -1 & -1 & 1 & 1 & -1 & -1 & 1 \\ 1 & 1 & -1 & -1 & -1 & -1 & 1 & 1 \\ 1 & -1 & 1 & -1 & 1 & -1 & 1 & -1 \\ 1 & -1 & 1 & -1 & -1 & 1 & -1 & 1 \\ 1 & -1 & -1 & 1 & 1 & -1 & -1 & 1 \\ 1 & -1 & -1 & 1 & -1 & 1 & 1 & -1 \end{vmatrix} \qquad (6)$$

Each row is represented by $O_{8, w}$, where w is the row number.

2.1.5 Orthogonal ZCPS

The pilot decontamination technique multiplies ZCPS element-wise with the individual orthogonal code rows to achieve orthogonality across the network. The technique chooses the length of ZCPS as the multiple of two (that is, $P=2^m$, $m \geq 2$).

Therefore, the ZC sequence with $P=2^m$ is written (Ali *et al.*, 2017) as:

$$Z_\mu(n) = e^{-j\pi\mu\frac{n}{2^m}^2}, n = 0,1, \dots . P - 1 \qquad (7)$$

The set of cyclically shifted version of Z_μ is represented by$Z_\mu(\Delta k)$, where, Δk is the cyclic shift (Ali *et al.*, 2017a) and expressed as:

$$-(2^m - 1) \leq \Delta k \leq (2^m - 1) \qquad (8)$$

Considering a system composing of seven cells, the separate orthogonal code row is given to each BS of the cluster of seven cells. The assigned distinct orthogonal code row is multiplied element-wise with the set of ZC sequence at the BS of the seven cells.

The result of the multiplication is given (Ali *et al.*, 2017) as:

$$C_{e,\Delta k} = Z_\mu(\Delta k) * O_{8,w} \qquad (9)$$

$$C_{e,\Delta k} = Z_\mu(n + \Delta k) * O_{8,w}(n + 1) \qquad (10)$$

where, $n = 0,1,\ldots,2^m - 1$, '$*$' represents the element-wise multiplication, and e=1, 2,…,7 denote the number of the BS in the seven cells.

2.1.6 Grouping User Terminals

For commonly used block fading model, it is assumed that the channel gain will remain steady during the coherence interval. Considering the k^{th}user, the j^{th} cell, and the i^{th} BS, the large-scale fading channel coefficient, δ_{ljk}, which is the same at the BS but dependent of Mobile Terminal (UT), is given by Zhou *et al.*, (2018) as follows:

$$\delta_{ijk} = \frac{\Lambda_{ijk}}{(r_{ijk}/r_{min})^{\gamma}} \qquad (11)$$

where, Λ_{ijk} is the shadow fading factor, r_{ijk}denotes the distance between user k of cell j to BS l,r_{min}represents the minimum distance between users and BS (cell radius), and γsignifies the path loss exponent. Therefore, for a UT, with$C$ denoting the center cell users and E the cell edge users.

$$a\ user\ is\ C\ if\ \delta_{ijk}^2 > \rho_l \qquad (12)$$

$$a\ user\ is\ E\ if\ \delta_{ijk}^2 \leq \rho_l \qquad (13)$$

where, ρ_l is the power threshold for the grouping, that is independent of geographic location of the UT, rather it depends on signal space of δ_{ijk} and can be expressed (Zhu *et al.*, 2016) as:

$$\rho_l = \frac{\lambda}{K}\sum_{k=1}^{K}\delta_{ijk}^2 \qquad (14)$$

where, $\rho_l$denotes the threshold adjustment parameter that can be tuned in accordance with system design, Krepresents the number of users, and δ_{ijk}^2 is the power based on large-scale fading coefficient. It is generally assumed that $\delta_{ijk}^2$is known at the BS (Zhu *et al.*, 2016).

The UTs are divided into center cell and edge cell users, respectively. The division is done based on large-scale fading coefficient because the achievable rate for M-MIMO depends on it (Yang *et al.*, 2015). The division made, improves the Quality of Service (QoS) of the edge users, thereby increasing the throughput of the system. The adjustment of λ determines a user as center cell or edge cell user. When the value of $\lambda$is zero, all users are edge cell users. On the other hand, when λ is set to the highest value of K, (that is, $\lambda = K$), implying that all the users are center cell users.

For a center cell pilot number $P_s \leq K_C$,the pilots with new users are shared if the following holds:

$$P_s = 0 \qquad (15)$$

That is, when the center cell pilot $P_s$are exhausted, pilot sharing with new users start. Otherwise, each user is assigned a pilot.

2.1.7 Center Cell Pilot Sharing

The center cell pilot sharing is achieved through the employment of Hadamard matrix that solves the problem of intra-cell interference caused by pilot sharing. Hadamard matrix is characterized as a square matrix that is the same as its inverse and whose elements are either 1 or -1 and orthogonal in nature. The Hadamard matrix is derived from OVSF (Rintakoski *et al.*, 2004), which is clarified mathematically as follows:

$$H_T = \begin{bmatrix} H & H \\ H & -H \end{bmatrix} \qquad (16)$$

3. METHODOLOGY AND SIMULATION

The methodology adopted in this research work involves a cellular network of L hexagonal cells in which the BS of each cell contains an array of$A$ antennae and serves U single antenna Mobile

Terminals (MTs) in the same frequency time resource considered.

Users were grouped into center cell users and edge cell users based on their large-scale fading coefficient.

Pilot Sequences (PSs) are assigned to users sequentially for the center cell users, but shared sequentially with other users when pilots are exhausted. The Hadamard code is assigned to the new user. OVSF codes are assigned to cell edge users and then multiply with ZCPS across the edge cells.

Minimum Mean Square Error (MMSE) estimator and linear equalizers are employed for Channel State Information (CSI) estimation and sum-rate capacity determination of the developed improved orthogonal uplink pilot sequence decontamination scheme. The system architecture of this developed scheme is shown in Figure 2.

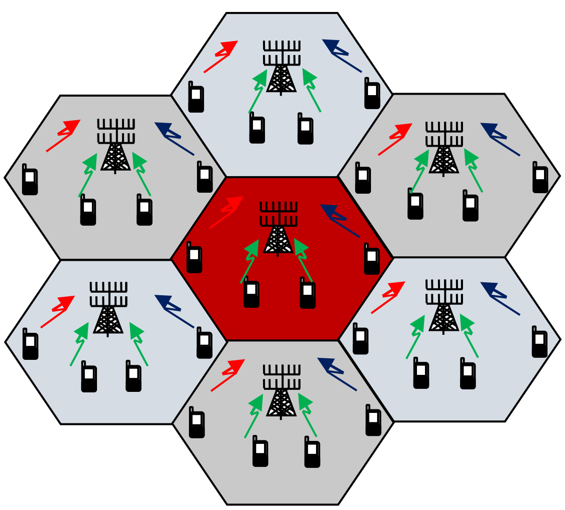

Figure 2: System Architecture of the Developed Decontamination Scheme

Sum-rate capacity is used as the performance metric for the validation and evaluation of the developed pilot decontamination scheme when compared with the work of the base paper.

4. RESULTS AND DISCUSSION

The results achieved from the improved pilot decontamination scheme using orthogonal uplink pilot sequence based on large-scale fading are presented. The scheme's performance was weighed up using sum-rate.

Parameter	Symbol	Value
Number of cells	L	7
Transmission Frequency	F	2100MHZ
Number of users per cell	U	13
Number of antennas	A	100
Average UL TX power	ρ_{up}	0dB
Average DL TX power	ρ_{up}	10dB
Direct gain	β_{qqu}	1
Cross gain	β_{lqu}	0.3
Pilot length	$P = 2^m$	8
Frequency reuse factor	φ	1
Mean of AOAs	x_{AOA}	90^0
Standard deviation of AOAs	σ_{AOA}	90^0
Antenna spacing	D	$\lambda/2$
Number of paths	t	100

The simulation results obtained based on the model parameter values shown in Table 1 for the developed scheme are discussed here. The technique was developed based on Nakagami Fading channel model. Figure 2 depicts the plots of sum-rate versus standard deviation of Angle of Arrivals (AoAs) of the two systems obtained using equation (2.11), where the AoAs ranges from 0^0 to 90^0. The performance of the developed scheme is represented in red and that of the existing scheme, Ali *et al.*, (2017a), in black. At 0^0 standard deviation of AoA, the existing scheme offers sum-rate capacity of 21bps while the developed scheme presents sum-rate capacity of 22bps. At 90^0 standard deviation of AoA, the existing scheme presents sum-rate capacity of 23.5bps while the developed scheme presents sum-rate capacity of 25bps, respectively. This shows that there is sum-rate capacity improvement of 1bps and 1.5bps at 0° and 90° standard deviation of AoA, respectively. The developed pilot decontamination scheme outperformed the scheme of Ali *et al*., (2017a) with better sum-rate capacity due to the reduction of interference caused by pilot contamination.

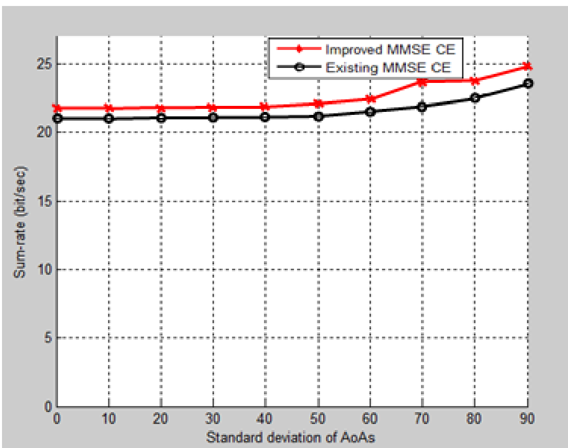

Figure 3: Sum-Rate versus Standard deviation of AOAs of Schemes

Figure 4 depicts the sum-rate versus the number of antennae performance of the existing and the developed pilot decontamination schemes, with number of antennae ranging from 0 to 100.

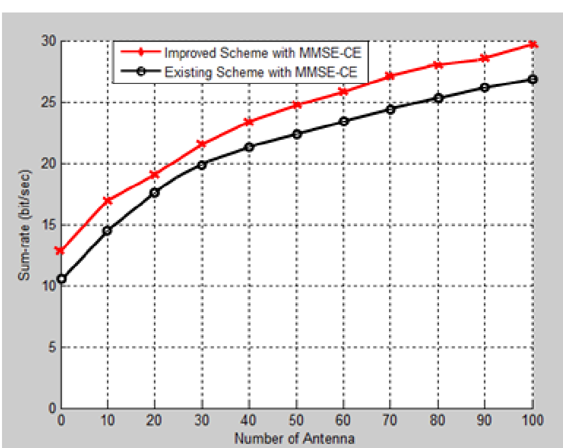

Figure 4: Sum-Rate versus Number of Antennae of Schemes

From the simulation results obtained, when the number of antennae is 0, the sum-rates for the existing and developed schemes are 10.5bps and 13bps, respectively. When the number of antennae is 100, the sum-rates for the existing and the developed schemes are 27bps and 30bps, respectively. This shows that the developed scheme outperformed the existing scheme with improvements of 2bps and 3bps at 0 and 100 numbers of antennae, respectively.

The results of the plot of Figure 4 obtained using equation (2.11) shows the comparison of the developed and Ali *et al*., (2017a) schemes when sum-rate is plotted against cross gain.

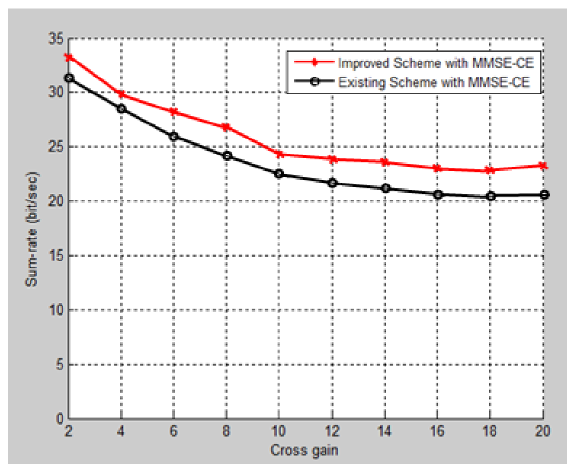

Figure 5: Sum-Rate versus Cross Gain of Schemes

At cross gain of 2, the sum-rates of both the existing and developed schemes are given by 31.5bps and 33bps, respectively while at the cross gain of 20, the sum-rates are given by 20.5bps and 23bps, respectively. This indicates improvements of 1.5bps and 2.5bps at cross gains of 2 and 20, respectively.

The sum-rate versus number of cell performance comparison of the two schemes is shown in Figure 6.

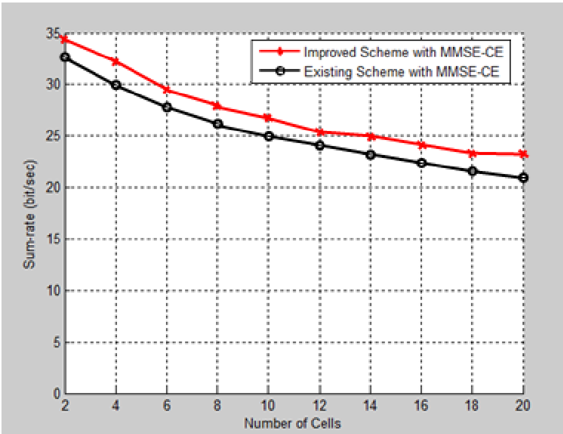

Figure 6: Sum-Rate verses Schemes Number of Cells

The sum-rate decreases for both the work of Ali *et al.,* (2017a) and that of the developed pilot decontamination schemes. When the number of cells is 2, the sum-rates for both the existing and the developed schemes are 32.6bps and 35bps, respectively while when the number of cells is 20, the sum-rates for both the existing and the developed schemes are 21bps and 23.2bps, respectively. This shows improvements of 2.4bps and 2.2bps, respectively. From results achieved, it is observed that the developed pilot decontamination scheme outperformed the existing pilot decontamination scheme implemented by Ali *et al*., (2017a) in terms of sum-rate capacity. The improvement is as a result of the reduction of inter-cell interference due to pilot contamination during the channel estimation process.

5. CONCLUSION

Pilot contamination during channel estimation process is a major challenge in Time Division Duplex (TDD) Massive Multiple Input Multiple Out (M-MIMO) systems because it limits the sum-rate capacity of the system. An improved pilot decontamination using orthogonal uplink pilot sequence based on large-scale fading M-MIMO system was developed. Users are grouped into center cell and edge cell users based on their large-scale fading. The cell center users were assigned set of pilots, which were shared with new users. The cell edge users were assigned distinct OVSF codes which were multiplied with Zadoff Chu Pilot Sequence (ZCPS). This multiplication created orthogonality across the edge cell users. After creating orthogonality among the cell center and cell edge users, successful pilot transmission that was free from contamination was achieved. When the developed pilot decontamination was compared with the existing work of Ali *et al*., (2017a), the developed scheme provided sum-rate capacity improvement of 1.5bps, 3bps, 2.5bps and 2.5bps when plotted against standard deviation of AoAs, number of antennae, cross gains and number of cells, respectively

REFERENCE

Albreem, M. A., Juntti, M., & Shahabuddin, S. (2019). Massive MIMO detection techniques: a survey. *IEEE Communications Surveys & Tutorials, 21*(4), 3109-3132.

Ali, S., Chen, Z., & Yin, F. (2017). Design of Orthogonal Uplink Pilot Sequences for TDD Massive MIMO under Pilot Contamination. *Journal of Communications, 12*(1).

Ali, S., Chen, Z., & Yin, F. (2017a). Pilot decontamination in TDD multicell massive MIMO systems with infinite number of BS antennas. *Canadian Journal of Electrical and Computer Engineering, 40*(3), 171-180.

Alsharif, M. H., & Nordin, R. (2017). Evolution towards fifth generation (5G) wireless networks: Current trends and challenges in the deployment of millimetre wave, massive MIMO, and small cells. *Telecommunication Systems, 64*(4), 617-637.

Benmimoune, M., Driouch, E., Ajib, W., & Massicotte, D. (2015). *Feedback reduction and efficient antenna selection for massive MIMO system.* Paper presented at the Vehicular Technology Conference (VTC Fall), 2015 IEEE 82nd.

Elijah, O., Leow, C. Y., Rahman, T. A., Nunoo, S., & Iliya, S. Z. (2016). A comprehensive survey of pilot contamination in massive MIMO—5G system. *IEEE Communications Surveys & Tutorials*, *18*(2), 905-923.

Fatema, N., Hua, G., Xiang, Y., Peng, D., & Natgunanathan, I. (2017). Massive MIMO linear precoding: A survey. *IEEE Systems Journal*(99), 1-12.

Ju, M., Xu, L., Jin, L., & Huang, D. D. (2017). *Data aided channel estimation for massive MIMO with pilot contamination.* Paper presented at the Communications (ICC), 2017 IEEE International Conference on.

Larsson, E. G., Edfors, O., Tufvesson, F., & Marzetta, T. L. (2014). Massive MIMO for next generation wireless systems. *IEEE communications magazine, 52*(2), 186-195.

Li, Q. C., Niu, H., Papathanassiou, A. T., & Wu, G. (2014). 5G network capacity: Key elements and technologies. *IEEE Vehicular Technology Magazine, 9*(1), 71-78.

Liu, Z., Du, W., & Sun, D. (2017). Energy and spectral efficiency tradeoff for massive MIMO systems with transmit antenna selection. *IEEE Transactions on Vehicular Technology, 66*(5), 4453-4457.

Marzetta, T. L., Larsson, E. G., Yang, H., & Ngo, H. Q. (2016). *Fundamentals of massive MIMO*: Cambridge University Press.

Mehrotra, N., & Chaubey, A. K. (2017). Pilot Contamination Effect in Massive MIMO and Analysis of Mitigation Techniques: February.

Muppirisetty, L. S., Charalambous, T., Karout, J., Fodor, G., & Wymeersch, H. (2018). Location-Aided Pilot Contamination Avoidance for Massive MIMO Systems. *IEEE Transactions on Wireless Communications, 17*(4), 2662-2674.

Rintakoski, T., Kuulusa, M., & Nurmi, J. (2004). *Hardware unit for ovsf/walsh/hadamard code generation [3g mobile communication applications].* Paper presented at the 2004 International Symposium on System-on-Chip, 2004. Proceedings.

Salh, A., Audah L., Shah, N. M., Hamzah, S. A., 2020 Mitigating Pilot Contamination for Channel. Estimation in Multi-cell Massive MIMO Systems. © SpringerScience+Business Media, LLC, part of Springer Nature

S. M. Waziri, M. B. Abdurrazaq, A. M. S. Tekanyi, A. Muhammad, H. A. Abdulkareem, (2019)" Pilot Contamination Effect Mitigation in Massive Multiple Input Multiple Output System and Analysis of Mitigation Techniques" Computing & Information Systems, Vol. 23 Issue 2, p35-46. 12p.

Tebe, P. I., Kuang, Y., Opare, K. A., & Kponyo, J. J. (2015). *The effect of channel estimation errors on the energy efficiency of downlink massive MIMO systems.* Paper presented at the Ubiquitous and Future Networks (ICUFN), 2015 Seventh International Conference on.

Tseng, Y.-C., & Chao, C.-M. (2002). Code placement and replacement strategies for wideband CDMA OVSF code tree management. *IEEE transactions on mobile computing, 99*(4), 293-302.

Yang, A., He, Z., Xing, C., Fei, Z., & Kuang, J. (2015). The role of large-scale fading in uplink massive MIMO systems. *IEEE Transactions on Vehicular Technology*, *65*(1), 477-483.

Yin, H., Gesbert, D., Filippou, M., & Liu, Y. (2013). A coordinated approach to channel estimation in large-scale multiple-antenna systems. *IEEE Journal on Selected Areas in Communications, 31*(2), 264-273.

Zhou, R., Fu, Y., & Wang, H. (2018). *Uplink Asynchronous Fractional Pilots Scheduling in Massive MIMO System.* Paper presented at the 2018 IEEE 18th International Conference on Communication Technology (ICCT).

Zhu, X., Wang, Z., Qian, C., Dai, L., Chen, J., Chen, S., & Hanzo, L. (2016). Soft Pilot Reuse and Multicell Block Diagonalization Precoding for Massive MIMO Systems. *IEEE Trans. Vehicular Technology*, *65*(5), 3285-3298.